AIMS Mathematics, 11(1): 578–593.
DOI: 10.3934/math.2026025
Received: 08 October 2025
Revised: 14 December 2025
Accepted: 29 December 2025
Published: 08 January 2026

https://www.aimspress.com/journal/Math

Research article

Dynamics of a predator-prey model with the Allee effect for the predator induced by weighted harvesting strategy

Jing Xu[1,*] **and Tao Zou**[2]

[1] School of Mathematics and Statistics, Hubei Normal University, Huangshi, 435002, China
[2] School of Artificial Intelligence and Computer Science, Hubei Normal University,Huangshi, 435002, China

* **Correspondence:** Email: Jingxumath@163.com.

Abstract: Over-exploitation of natural resources poses cascading challenges to the environment, economy, and public health. To mitigate these adverse impacts and achieve long-term ecological and socioeconomic balance, sustainable development strategies are imperative. Thus, in this paper, we developed a predator-prey model with state-dependent impulsive control, grounded in the weighted escapement policy, to regulate resource harvesting more realistically. We investigated the model's dynamical behaviors, focusing on the existence and stability of semi-trivial and order-1 periodic solutions. To enhance economic viability while ensuring sustainability, an optimization problem was formulated to maximize long-term profits via optimal harvesting schemes. Finally, numerical simulations validated the theoretical results, quantified the optimal harvesting level and weight parameter of the weighted escapement policy, and provided actionable insights for practical resource management.

Keywords: Allee effect; weighted harvesting strategy; periodic solution; orbital stability; optimization
Mathematics Subject Classification: 92D25, 92D40

1. Introduction

The Allee effect is described as a decrease in the per capita population growth rate at low numbers of the population density [1]. Courchamp et al. [2] showed that the population dynamics can be modified when there is an Allee effect, such as leading to long-term transients phenomena [3]. Inspired by Allee [4], ecological studies classify this effect into additive [5–7] and multiplicative [8–10] types, both of which are explored for their dynamical properties, such as mathematical traits, expression in population models, ecological impacts, and regulatory effects on extinction risk and system stability.

Additional forms exist as well; Zu and Mimura [11], for instance, linked fertility to population size via the Allee effect and found it elevates species extinction risk. With distinct mathematical expressions documented, these studies provide a theoretical basis for building predator-prey models that integrate the Allee effect.

However, inspired by the ideas of [12–14], Sen et al. [15] developed the following predator-prey model with a general case of Allee effect in the predator:

$$\begin{cases} \frac{\mathrm{d}x(t)}{\mathrm{d}t} = rx(t)\left(1 - \frac{x(t)}{K}\right) - \frac{ax(t)y(t)}{1+aqx(t)}, \\ \frac{\mathrm{d}y(t)}{\mathrm{d}t} = e\psi(y)\frac{ax(t)y(t)}{1+aqx(t)} - \mu y(t), \\ x(0) = x_0, y(0) = y_0, \end{cases} \tag{1.1}$$

where $x(t)$ and $y(t)$ represent the densities of prey and predator, respectively, and $(x(0), y(0)) = (x_0, y_0)$ is the positive initial value. r is the intrinsic growth rate of the prey, and K is the environment capacity. e $(0 < e < 1)$ is the maximum food conversion coefficient, and μ represents the death rate of the predator. The function $\psi(y)$ is used to describe the Allee effect in the predator, which has the following properties:

(1) $\psi(0) = 0$, $0 \leq \psi(y) \leq 1$, for large y, there is $\psi(y) \to 1$;

(2) $\psi(y)$ is an increasing function of y, thus there is $\psi'(y) > 0$ for all $y \geq 0$;

(3) $\psi''(y) < 0$ for all $y \geq 0$.

The authors investigated the existence of local bifurcations, such as Hopf, generalized Hopf, and Bogdanov-Takens bifurcations, and studied the influence of different forms of the Allee effect on the dynamics of model (1.1).

Predator-prey interactions are at the core of ecosystem stability. Therefore, formulating effective population regulation and sustainable resource utilization strategies is an urgent task. Overexploitation of natural resources has caused severe environmental degradation; for example, the International Whaling Commission (IWC) set annual catch quotas and decided on a total ban on commercial whaling due to the decline in whale numbers caused by overfishing [16]. Due to the needs of business and livelihood, the exploitation and utilization of resources is inevitable. Thereafter, how human populations might best manage the natural resources to sustain a yield for human without exterminating species is discussed. To address this, scholars came up with different harvesting strategies, including continuous time harvesting [17, 18], threshold harvesting [19, 20], and impulsive harvesting [21, 22]. The weighted escapement policy (WEP), proposed by [23, 24], has emerged as a promising tool for population management. For example, Costa et al. [25] investigated the dynamics of the Lotka-Volterra model and Leslie-Gower model subjected to the WEP, respectively, and the obtained results could contribute to assessing the effect of the WEP. Notably, Tian et al. [26–28] investigated the dynamics of three types of predator-prey fishery models guided by the WEP, and the profits of the harvesting process was formulated. By solving the optimization problem, the optimal capture and the weight are determined. Despite these advances, one key aspect has not been fully explored in the literature. While Tian et al. [26–28] established a solid theoretical foundation for WEP-based predator-prey system management, their framework does not incorporate the general Allee effect in predator populations, a critical ecological mechanism that modulates population dynamics, especially at low predator densities. To address this unexamined combination, in this paper, we construct a predator-prey

model coupling the general predator Allee effect proposed by Sen et al. [15] with the classic WEP, and systematically investigate the system's dynamical behaviors and optimal management strategies.

The novelty of this paper is as follows: (1) A predator-prey model with the Allee effect in the predator induced by the WEP is developed; and (2) the corresponding optimization problem is formulated and solved. The structure of this paper is as follows: In Section 2, we present a predator-prey model with the Allee effect in the predator induced by the WEP, and investigate the dynamics of the proposed model, including the existence and stability of the semi-trivial and positive order-1 periodic solution. In Section 3, we verify the theoretical results and determine the optimal harvesting level and weight via numerical simulations. Finally, we give a brief conclusion.

2. Model formulation and major results

In this section, we introduce the dynamical behavior of system (1.1) and formulate the corresponding impulsive differential equation. In the following, we summarize the dynamics of system (1.1).

2.1. Dynamics of system (1.1)

After a simple calculation, we find that the isoclinic line $l_3 := \{(x,y)|r - \frac{rx}{K} - \frac{ay}{1+aqx} = 0\}$ has a horizontal asymptote $l_2 := \{(x,y)|y = \psi^{-1}(\frac{\mu q}{e})\}$ and a vertical asymptote $l_1 := \{(x,y)|x = \frac{\mu}{e-\mu q}\}$, respectively. The other isoclinic line $l_4 := \{(x,y)|\psi(y)\frac{eax}{1+aqx} - \mu = 0\}$ exists as a unique extreme point (x_m, y_m) (see Figure 1). The existence and stability of feasible equilibrium points are listed by the following two lemmas:

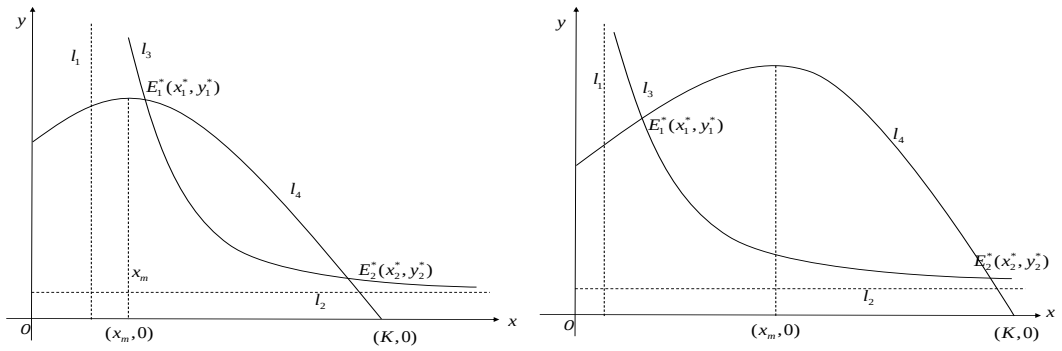

Figure 1. The location relationship between x_1^* and x_m: (a) $x_m < x_1^* < K$; (b) $x_1^* < x_m < K$.

Lemma 2.1. *[15] For any $\psi(y)$ with the properties (1)–(3) in model* (1.1)*, $E_0(0,0)$ is a saddle, and $E_1(K,0)$ is locally asymptotically stable.*

Lemma 2.2. *[15] For case of $x_m < x_1^* < x_2^* < K$, if $-\frac{r}{K} + \frac{a^2qy_1^*}{(1+aqx_1^*)^2} + e\psi'(y_1^*)\frac{ax_1^*}{1+aqx_1^*} < 0$, E_1^* is locally asymptotically stable (see Figure 1(a)); for the case of $x_1^* < x_m < x_2^* < K$, there is $-\frac{r}{K} + \frac{a^2qy_1^*}{(1+aqx_1^*)^2} + e\psi'(y_1^*)\frac{ax_1^*}{1+aqx_1^*} > 0$. Thus, E_1^* is unstable (see Figure 1(b)). E_2^* is always a saddle point.*

2.2. Dynamics of harvesting model (2.1)

In the following, we construct the model with harvesting strategy. Let η be the harvesting weight of the prey and $1-\eta$ be the harvesting weight of the predator. Since over-exploitation of natural resources has caused a lot of problems, from the perspective of resource conservation, when the sum of weights of two population densities reaches a certain condition, which is denoted by h_l, the harvesting strategy is adopted. In addition, due to the Allee effect in the predator, when harvesting strategy is adopted, it is necessary to release the immature predator to maintain the permanence of the predator population. Then, we have the following harvesting model:

$$\begin{cases} \left.\begin{array}{l} \frac{\mathrm{d}x}{\mathrm{d}t} = rx(t)(1-\frac{x(t)}{K}) - \frac{ax(t)y(t)}{1+aqx(t)}, \\ \frac{\mathrm{d}y}{\mathrm{d}t} = e\psi(y)\frac{ax(t)y(t)}{1+aqx(t)} - \mu y(t), \end{array}\right\} & \eta x + (1-\eta)y < h_l, \\ \left.\begin{array}{l} \Delta x = -p_1 E_l x, \\ \Delta y = -p_2 E_l y + \tau_l, \end{array}\right\} & \eta x + (1-\eta)y = h_l. \end{cases} \tag{2.1}$$

The model sets species-specific pulse terms for prey-predator harvesting and immature predator supplementation. The prey term $\Delta x = -p_1 E_l x$ regulates prey density within a sustainable range via proportional harvesting, where p_1 denotes prey harvesting efficiency and E_l represents the unified harvesting effort applied to both species. The predator term $\Delta y = -p_2 E_l y + \tau_l$ offsets harvesting-induced losses with immature predator release: p_2 is the predator harvesting efficiency, and the positive constant τ_l quantifies the number of immature predators supplemented during each harvesting event. This dual-design pulse system is critical to prevent Allee-effect-vulnerable predators from falling to a growth-limiting density and maintain trophic stability. The WEP threshold $h_l = \eta x + (1-\eta)y$ reflects the inherent trophic interdependence of prey and predator populations, moving beyond single-species threshold limitations. The adjustable η enables flexible prioritization: Higher values favor prey conservation for predator food supply, lower values prioritize predator persistence. This design avoids the ecological risks of isolated species management and provides a holistic framework for sustainable population control.

In the following, we mainly investigate the dynamical behavior of system (2.1), including the existence and stability of the semi-trivial periodic solution and the order-1 periodic solution.

For system (2.1), we define impulsive set and phase set respectively as follows:

$$M_{Imp} = \{(x, y) | 0 \le x \le K, \eta x + (1-\eta)y = h_l\},$$

and

$$N_{Pha} = \left\{(x, y) | \frac{\eta x}{1-p_1 E_l} + \frac{(1-\eta)y}{1-p_2 E_l} = h_l + \frac{(1-\eta)\tau_l}{1-p_2 E_l}\right\}.$$

2.2.1. The semi-trivial periodic solution

For system (2.1), if $\tau_l = 0$, $y(0) = 0$, then there is $y(t) \equiv 0$. If $h_l \le \eta K$, then system (2.1) becomes the following subsystem:

$$\begin{cases} \left.\begin{array}{l} \frac{\mathrm{d}x}{\mathrm{d}t} = rx(t)(1-\frac{x(t)}{K}), \\ y = 0, \end{array}\right\} & x < h_l/\eta, \\ \left.\begin{array}{l} \Delta x = -p_1 E_l x, \\ \Delta y = 0, \end{array}\right\} & x = h_l/\eta. \end{cases} \tag{2.2}$$

The intersection point of phase set N_{Pha} and the x-axis results in $x_0 = (1 - p_1E_l)h_l/\eta$. Define $x(t) = \overline{x}(t)$ as the solution of the equation $\frac{\mathrm{d}x}{\mathrm{d}t} = rx(t)\left(1 - \frac{x(t)}{K}\right)$ with $x(0) = x_0$. Thus, $(\overline{x}(t), 0)$ is the solution of system (2.2). Define $T = \frac{1}{r}\ln\left(\frac{K-(1-p_1E_l)h_l/\eta}{(1-p_1E_l)(K-h_l/\eta)}\right)$, which quantifies the time interval between two consecutive impulsive harvesting events. Then, we have $\overline{x}(T) = h_l/\eta$ and $\overline{x}(T^+) = x_0$. This means that $x(t) = \overline{x}(t), (n-1)T < t \le nT, n \ge 1$ is a periodic solution of system (2.2).

Theorem 2.1. *If $\tau_l = 0$ and $x \le h_l/\eta$, then system* (2.1) *exists as a semi-trivial periodic solution* $(\overline{x}(t), 0)$*, and it is orbitally asymptotically stable in the case of $p_2 > \overline{p}_2$, where*

$$\overline{p}_2 = \frac{p_1h_l}{\eta K - (1 - p_1E_l)h_l}.$$

Proof. Based on Lemma 2.1, we know that $(K, 0)$ is asymptotically stable. Thus, for the case of $h_l > \eta K$, system (2.2) does not have a periodic solution. Assume that there is a point $C(x_C, 0)$, which is the intersection point of the phase set N_{Pha} and x-axis (see Figure 2).

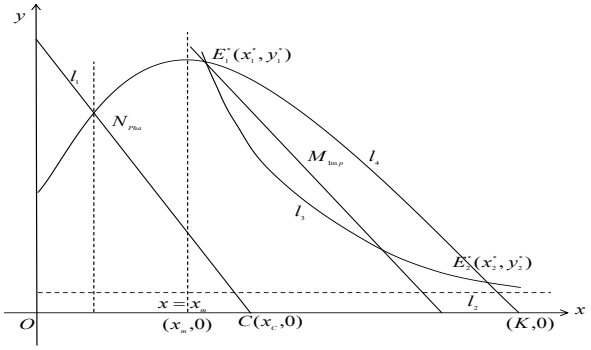

Figure 2. The existence of the semi-trivial order-1 periodic solution.

For the case of $h_l \le \eta K$, based on the definition of the type-I successor function, there is $f^I_{Sor}(C) = 0$. For system (2.2), we have

$$F(x,y) = rx(1 - x/K) - \frac{axy}{1 + aqx},\ G(x,y) = e\psi(y)\frac{axy}{1 + aqx} - \mu y,$$
$$\phi(x,y) = -p_1E_lx,\ \varphi(x,y) = -p_2E_ly,\ \zeta(x,y) = \eta x + (1 - \eta)y.$$

After a simple calculation, we have

$$\frac{\partial F}{\partial x} = r - \frac{2rx}{K} - \frac{ay}{(1 + aqx)^2},\ \frac{\partial G}{\partial y} = e\psi'(y)\frac{axy}{1 + aqx} + e\psi(y)\frac{ax}{1 + aqx} - \mu,$$
$$\frac{\partial \phi}{\partial x} = -p_1E_l,\ \frac{\partial \phi}{\partial y} = 0,\ \frac{\partial \varphi}{\partial x} = 0,\ \frac{\partial \varphi}{\partial y} = -p_2E_l,\ \frac{\partial \zeta}{\partial x} = \eta,\ \frac{\partial \zeta}{\partial y} = 1 - \eta.$$

Then

$$\begin{aligned}\Delta_1 =& \frac{F^I_+(\frac{\partial \varphi}{\partial y}\frac{\partial \zeta}{\partial x} - \frac{\partial \varphi}{\partial y}\frac{\partial \zeta}{\partial y} + \frac{\partial \zeta}{\partial x}) + G^I_+(\frac{\partial \phi}{\partial y}\frac{\partial \zeta}{\partial x} - \frac{\partial \phi}{\partial y}\frac{\partial \zeta}{\partial y} + \frac{\partial \zeta}{\partial x})}{F^I(\frac{\partial \zeta}{\partial x}) + G^I(\frac{\partial \zeta}{\partial y})}\\ =& \frac{(r(1 - p_1E_l)h_l/\eta)(1 - (1 - p_1E_l)h_l/(K\eta))(\eta - p_2E_l\eta)}{rh_l/\eta(1 - h_l/(K\eta))\eta}\\ =& (1 - p_1E_l)(1 - p_2E_l)\frac{\eta K - (1 - p_1E_l)h_l}{\eta K - h_l},\end{aligned}$$

and

$$\int_0^T \left(\frac{\partial F}{\partial x} + \frac{\partial G}{\partial y}\right)_{(\overline{x}(t),0)} \mathrm{d}t = \int_{(1-p_1E_l)h_l/\eta}^{h_l/\eta} \frac{1}{x}\mathrm{d}x + \int_0^T \left(-\frac{rx}{K} - \mu\right)\mathrm{d}t.$$

Thus, the convergency ratio ρ_1 is

$$\rho_1 = (1 - p_2E_l)\frac{\eta K - (1 - p_1E_l)h_l}{\eta K - h_l} \exp\left\{\int_0^T \left(-\frac{rx}{K} - \mu\right)\mathrm{d}t\right\}.$$

Based on biologically feasible assumptions ($p_1, p_2, E_l, \eta, K, h_l, r, \mu > 0$; $\eta K > h_l$; $1 - p_2E_l > 0$), the integrand $-\frac{rx}{K} - \mu < 0$ for all $t \in [0, T]$, yields $0 < \exp\left\{\int_0^T \left(-\frac{rx}{K} - \mu\right)\mathrm{d}t\right\} < 1$. Thus, a sufficient condition for $\rho_1 < 1$ is $(1 - p_2E_l)^{\frac{\eta K-(1-p_1E_l)h_l}{\eta K-h_l}} < 1$. Rearranging this inequality gives the constraint $p_2 > \frac{p_1h_l}{\eta K-(1-p_1E_l)h_l}$, which is sufficient but not necessary due to the exponential term's attenuation effect. Then we define the critical threshold $\overline{p}_2 = \frac{p_1h_l}{\eta K-(1-p_1E_l)h_l}$.

In case of $p_2 > \overline{p}_2$, there is $\rho_1 < 1$. Therefore, $(\overline{x}(t), 0)$ is orbitally asymptotically stable (OAS); if $p_2 < \overline{p}_2$, there is $\rho_1 > 1$, thus, $(\overline{x}(t), 0)$ is unstable.

Remark 2.1. *Theorem 2.1 reveals that when the capture rate (p_2) of the predator exceeds a critical threshold, the predator population will go extinct, which in turn causes the ecosystem to lose its persistence. This result theoretically confirms that over-harvesting of predators, i.e., over-exploitation of biological resources, directly disrupts ecological balance and poses a significant threat to the stable survival of the ecosystem.*

2.2.2. Existence and stability of the order-1 periodic solution

In the following, we mostly investigate the existence and stability of the order-1 periodic solution. For convenience, we define

$$\eta^* = \frac{y_1^*}{K - x_1^* + y_1^*},\ h^* = \eta x_1^* + (1 - \eta)y_1^*,$$
$$h_\tau^\eta = \max\{h_l | \eta x_{M_{Imp}} + (1 - \eta)y_{M_{Imp}} \geq h_l\}.$$

Theorem 2.2. *If one of the following three conditions holds, then system* (2.1) *has an order-1 periodic solution: (1)* $\tau_l = 0,\ h_l \leq \min\{h^*, \eta K\},\ p_2 < \overline{p}_2$*; (2)* $\tau_l = 0,\ \eta < \eta^*,\ \eta K < h_l \leq h_\tau^\eta$*; (3)* $0 < \tau_l,\ h_l \leq h_\tau^\eta$.

Proof. For case (1), the semi-trivial periodic solution is unstable. Assume that line l_5 is parallel to the x-axis, point H is the intersection of curve l_3 and the impulsive set M_{Imp}, and H_1 is a point in the neighborhood of H. By the properties of deterministic system (2.1), H_1 is the minimum point of curve l_6. Assume that the trajectory staring from point $A \in N_{Pha}$ intersects the impulsive set M_{Imp} at A^- with $y_{A^-} > y_A$, and jump into N_{Pha} at A^+ (see Figure 3(a)). If the successor point A^+ is below point A, then there is a semi-trivial periodic solution, which contradicts condition (1). Then by the definition of the successor function, we have

$$f_{Sor}^I(A) = d(A^+, C) - d(A, C) > 0.$$

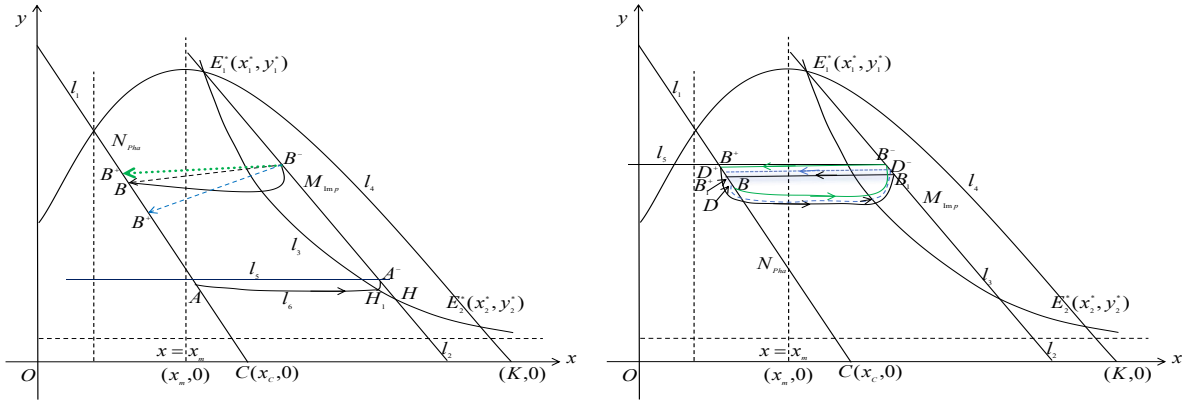

Figure 3. The existence of the order-1 periodic solution.

Assume that the trajectory starting from $B(x_B, y_B)$ intersects the impulsive set M_{Imp} at $B^-(x_{B^-}, y_{B^-})$, then jumps to the phase set N_{Pha} at B^+. There exist three cases:

(1) If the successor point of B overlaps point B, there is $f^I_{Sor}(B) = 0$, and $\overset{\frown}{BB^-B}$ forms an order-1 periodic solution.

(2) If the successor point B^+ is below B, then $f^I_{Sor}(B) < 0$ holds, thus there exists one point $L \in N_{Pha} \cap \overline{BA}$ such that $f^I_{Sor}(L) = 0$, meaning that system (2.1) has an order-1 periodic solution (see Figure 3(a)).

(3) For the case of that the successor point B^+ is above B, we need to use the type-II successor function. The trajectory passing through point B^+ passes through the phase set N_{Pha}, and intersects the impulsive set at B_1, then jumps to B_1^+ on N_{Pha}. Based on the property of system (2.1), we can conclude that point B_1 is below B^-, and B_1^+ is below B^+. Thus, we have

$$f^{II}_{Sor}(B^+) = d(B_1^+, C) - d(A^+, C) < 0.$$

In the following, we prove that there exists a point D such that $f^{II}_{Sor}(D) > 0$ (see Figure 3(b)). For a fixed $\varepsilon = d(B, B^+)/2$, there exists $\delta < \varepsilon$, for $D \in N_{Pha} \cap U(B, \delta)$ with $x_B < x_D$ and $y_B > y_D$, which holds that $d(D^-, B^-) < \varepsilon$. Then we have

$$\begin{aligned} d(D^+, B^+) &= \sqrt{(x_{D^+} - x_{B^+})^2 + (y_{D^+} - y_{B^+})^2} \\ &= \sqrt{((1 - p_1E_l)x_{D^-} - (1 - p_1E_l)x_{B^-})^2 + ((1 - p_2E_l)y_{D^-} - (1 - p_1E_l)y_{B^-})^2} \\ &\le \max\{(1 - p_1E_l), (1 - p_2E_l)\} d(D^-, B^-) < \varepsilon. \end{aligned}$$

Thus,

$$\begin{aligned} f^{II}_{Sor}(D) &= d(D^+, C) - d(D, C) \\ &= d(B^+, C) - d(B^+, D^+) - (d(B, C) + d(D, B)) \\ &= d(B^+, B) - (d(B^+, D^+) + d(D, B)) > 0. \end{aligned}$$

Then, there exists a point $L \in \overline{BB^+}$, satisfying $f^{II}_{Sor}(L) = 0$.

For cases (2) and (3), similar to the proof process of Theorem 2.2, there exists an order-1 periodic solution for system (2.1). This completes the proof.

Remark 2.2. *Theorem 2.2 reveals that when the capture rate (p_2) for the predator is controlled within a reasonable range, the ecosystem can maintain its persistence. Furthermore, if specific additional conditions are satisfied, the system will also exhibit periodic dynamic changes. This theoretical result not only clarifies the effective regulation range of the capture rate but also provides a solid mathematical basis for the sustainable development and management of biological resources.*

In the following, we prove the stability of the order-1 periodic solution. Assume that $(\widetilde{x}(t), \widetilde{y}(t))$ is an order-1 periodic solution of system (2.1) with period T_1.

Define

$$\begin{aligned}
&\tilde{x}_1 = \tilde{x}(T_1),\ \tilde{y}_1 = \tilde{y}(T_1),\ \tilde{x}_0 = (1 - p_1E_l)\tilde{x}_1,\ \tilde{y}_0 = (1 - p_2E_l)\tilde{y}_1 + \tau_l,\\
&\tilde{F}_0 = F(\tilde{x}_0,\ \tilde{y}_0),\ \tilde{G}_0 = G(\tilde{x}_0,\ \tilde{y}_0),\ \tilde{F}_1 = F_1(\tilde{x}_1,\ \tilde{y}_1),\ \tilde{G}_1 = G(\tilde{x}_1,\ \tilde{y}_1),\\
&\Phi = \ln\left\{\frac{(1 - p_1E_l)[(1 - p_2)E_l\tilde{y}_1 + \tau_l][\eta\tilde{F}_1 + (1 - \eta)\tilde{G}_1]}{\tilde{y}_1[\eta(1 - p_2E_l)\tilde{F}_0 + (1 - \eta)(1 - p_1E_l)\tilde{G}_0]}\right\}.
\end{aligned}$$

Theorem 2.3. *If there is*

$$\int_0^{T_1}\left(-\frac{rx(t)}{K} + \frac{ay(t)}{(1 + aqx(t))^2} + \frac{e\psi'(y)ax(t)y(t)}{1 + aqx(t)}\right)\mathrm{d}t < \Phi, \tag{2.3}$$

then the order-1 periodic solution $(\tilde{x}(t), \tilde{y}(t))$ is orbitally asymptotically stable.

Proof. By the same manner used in Theorem 2.1, we have

$$\Delta_1 = \frac{\eta(1 - p_2E_l)\tilde{F}_0 + (1 - \eta)(1 - p_1E_l)\tilde{G}_0}{\eta\tilde{F}_1 + (1 - \eta)\tilde{G}_1},$$

and

$$\begin{aligned}
&\exp\left\{\int_0^{T_1}\left(\frac{\partial F}{\partial x} + \frac{\partial G}{\partial y}\right)_{(\tilde{x}_1,\tilde{y}_1)}\mathrm{d}t\right\}\\
=&\frac{1}{(1 - p_1E_l)}\frac{\tilde{y}_1}{(1 - p_2)E_l\tilde{y}_1 + \tau_l}\exp\left\{\int_0^{T_1}\left(-\frac{rx(t)}{K} + \frac{ay(t)}{(1 + aqx(t))^2} + \frac{e\psi'(y)ax(t)y(t)}{1 + aqx(t)}\right)\mathrm{d}t\right\}.
\end{aligned}$$

If inequality (2.3) holds, then $|\rho_2| < 1$, and the order-1 periodic solution $(\tilde{x}(t), \tilde{y}(t))$ is orbitally asymptotically stable.

2.3. Optimal harvesting strategy

By Theorem 2.2, we can conclude that system (2.1) has an order-1 periodic solution if one of the three cases holds. Thus, the harvesting strategy can be considered. Let $x_l \in [x_1, x_2]$ be the target density of the prey and $y_l = \omega x_l$ be that of the predator. Assume that E_l depends on x_l and h_l, and τ depends on η and x_l. We also assume that $h_l = \eta x_l + (1 - \eta)y_l$, $E_l = E_1 + \frac{(x_l - x_1)E_2}{x_2 - x_1}$, $\tau_l = \tau_1 + \frac{(x_l - x_1)\tau_2}{x_2 - x_1}$. We can find that period T_1 depends on η and x_l. To maintain the persistence of the two populations and get maximum profits, we need to choose the optimal harvesting strategy. Let a_1 and a_2 represent the price on sale for the unit biomass of the prey and predator, respectively, a_3 be the cost per unit capture strength, and a_4 be the cost of unit biomass for feeding predators. Then the profits and be given by

$$\Psi_{Pro}(\eta, x_l) = a_1p_1E_l\tilde{x}_1 + a_2p_2E_l\tilde{y}_1 - a_3E_l - a_4\tau_l.$$

Our goal is to maximize the profits over a cycle, i.e.,

$$\max \frac{\Psi_{Pro}(\eta, x_l)}{T_1(\eta, x_l)}$$
$$s.t.\ \ x_l \in [x_1, x_2],\ \eta \in [0, 1].$$

By solving the above optimization problem, we can obtain the optimal capture level x_l^* and the optimal weight η^*. Moreover, we can get the optimal release of immature predators τ^* and the optimal capture strength E^* and the optimal capture period T_1^*. The results are dependent on the parameters $a_i, i = 1, 2, 3, 4$.

3. Numerical simulations and optimization

In this section, we perform some numerical simulations to demonstrate the obtained results. As presented in [15], there exist some concrete forms of $\psi(y)$ such as $\psi(y) = \frac{y}{\delta+y}$ (Monod type), $\psi(y) = 1 - e^{-\frac{y}{\delta}}$ (Ivlev type), and $\psi(y) = \tanh\frac{y}{\delta}$ (hyperbolic tangent type). In this section, to facilitate the numerical simulations, we choose a special case of the Allee effect as $\psi(y) = \frac{y}{\delta+y}$.

Example 3.1. To verify the existence of a semi-trivial periodic solution, we choose the model parameters as follows: $r = 2$, $K = 100$, $a = 0.3$, and $q = 0.39$, $\mu = 1$, $e = 0.45$, and $\delta = 0.1$, and control parameters $\eta = 0.6$, $h_l = 30$, $p_1 = 0.3$, $p_2 = 0.2$, $E_l = 2$; then, $h_l < \eta K = 60$ and $\overline{p}_2 = 0.1875 < p_2$. Based on Theorem 2.1, system (2.1) exists as a semi-trivial periodic solution. From Figure 4, we find that the population $x(t)$ changes periodically, and population $y(t)$ tends to be extinct. This means that the semi-trivial periodic solution is OAS.

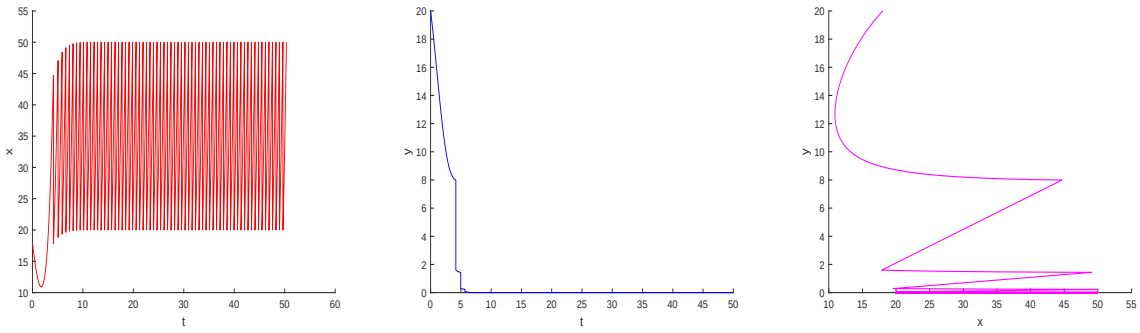

Figure 4. The existence of a semi-trivial periodic solution with $h_l < \eta K = 60$ and $\overline{p}_2 = 0.1875 < p_2$.

If $p_2 < \overline{p}_2$, then the semi-trivial periodic solution will lose its stability, and system (2.1) may exist as a positive periodic solution. This, we keep other parameters fixed but $\eta = 0.3$, $p_1 = 0.2$, $p_2 = 0.01$. By simple calculations, we can deduce that $(x_1^*, y_1^*) = (57.5171, 21.8914)$ is locally asymptotically stable, and $h^* = 0.3x_1^* + 0.7y_1^* = 32.5791$, $p_2 < \overline{p}_2 = 0.167$, then $h_l = 30 \leq \{\eta K, h^*\}$ is satisfied, corresponding to case (1) in Theorem 2.2, and system (2.1) exists as an order-1 periodic solution (see Figure 5).

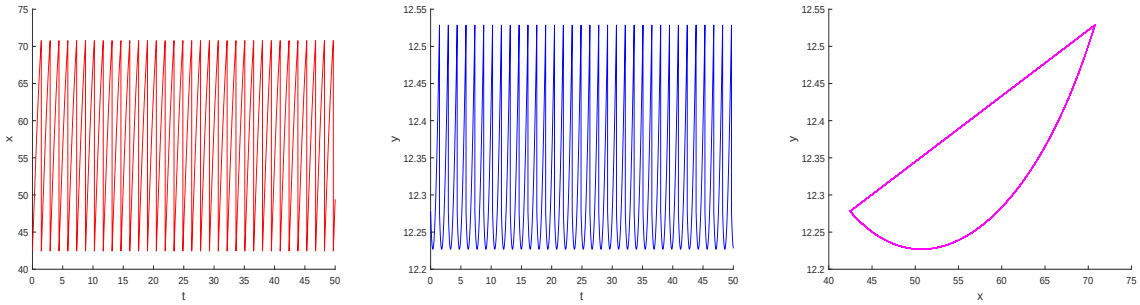

Figure 5. The existence of an order-1 periodic solution for case (1) in Theorem 2.2.

Example 3.2. To verify case (2) in Theorem 2.2, we choose $\tau = 0$, $h_l = 30$, $\eta = 0.1$, $p_1 = 0.2$, $E_l = 2$, and $p_2 = 0.01$ and keep other parameters unchanged. Thus, we have $\eta^* = \frac{y_1^*}{K - x_1^* + y_1^*} = 0.34$, $h_\tau^\eta = 63.6884$, so $\eta K < h_l < h_l^\eta$, $\eta < \eta^*$ is satisfied. From Figure 6, we find that the populations $x(t)$ and $y(t)$ change periodically. This shows that system (2.1) exists as an order-1 periodic solution for case (2) in Theorem 2.2.

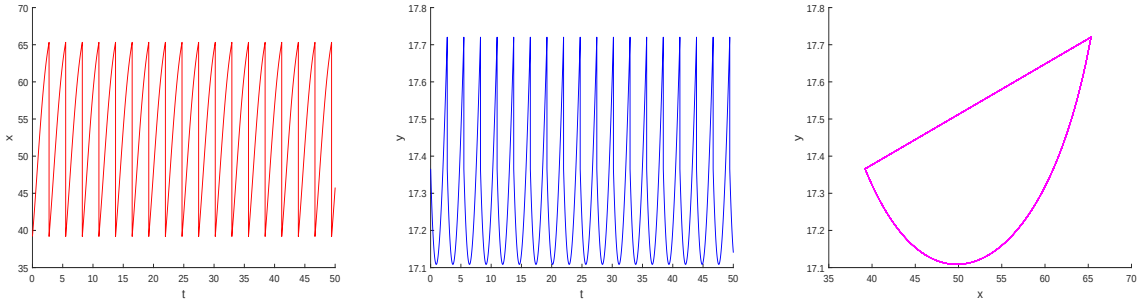

Figure 6. The existence of the order-1 periodic solution for case (2) in Theorem 2.2.

Example 3.3. For case (3) in Theorem 2.2, we choose that $\tau = 2$, $h_l = 32$, $\eta = 0.3$, $p_1 = 0.2$, $p_2 = 0.1$, and $E_l = 2$, so $h_l < h_l^\eta = 63.5129$ is satisfied. From Figure 7, we find that the populations $x(t)$ and $y(t)$ change periodically, indicating that system (2.1) exists as an order-1 periodic solution for case (3) in Theorem 2.2.

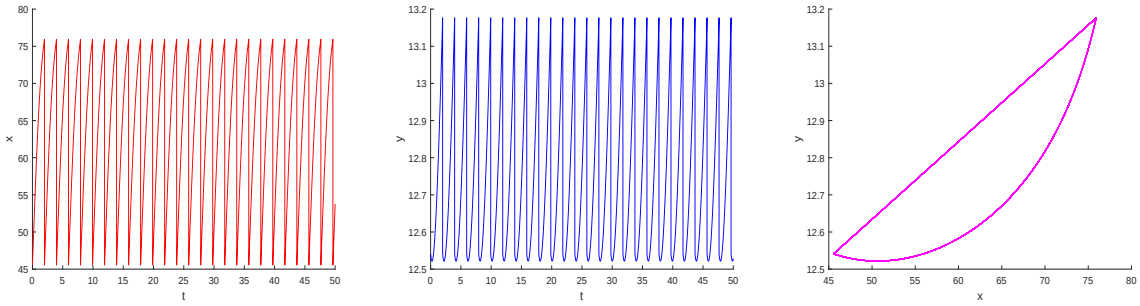

Figure 7. The existence of the order-1 periodic solution for case (3) in Theorem 2.2.

Example 3.4. Now, we determine the optimal harvesting level and optimal weight. Let $x_1 = 10$, $x_2 = 30$, $p_1 = 0.3$, $p_2 = 0.1$, $E_1 = 0.4$, $E_2 = 1$, $\tau_1 = 0.1$, $\tau_2 = 2.4$, and $r = 1.2$ with other model parameters unchanged. Then the $\tilde{x}_1$ with respect to η and x_l is listed in Figure 8(a), from which we can observe that $\tilde{x}_1$ is decreasing with the change of η for a given x_l, and increasing with the change of x_l for a given η.

For $a_1 = 10$, $a_2 = 250$, $a_3 = 100$, and $a_4 = 50$, the profit Ψ_{Pro} with respect to η and x_l is presented in Figure 8(b), from which we can observe that Q_{profit} achieves its maximum value at $\eta^* = 0.1$ and $x_l^* = 25$. In addition, the optimal weight η^* and the optimal harvesting level x_l^* depend on the values of the parameters a_i, $i = 1, 2, 3, 4$.

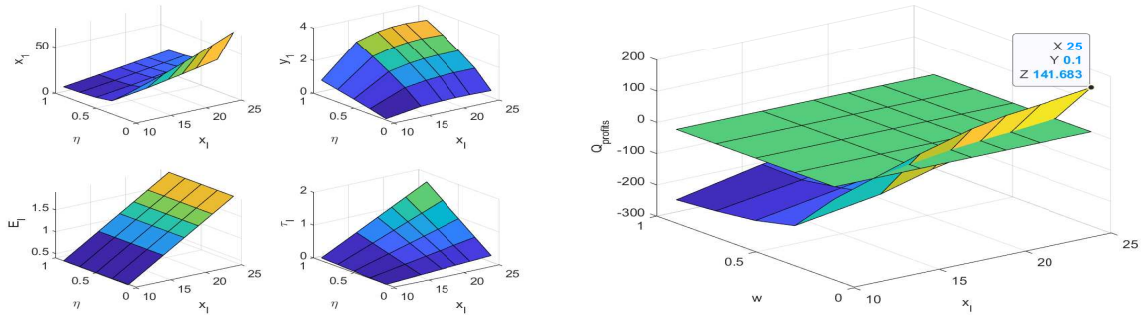

(a) (b)

Figure 8. The harvesting level x_l and profit Ψ_{Pro} with respect to η and x_1.

We now quantify the impact of model parameters on the profit (Q_{profit}) via numerical simulations. We choose $K = 100$, $a = 0.3$, $q = 0.39$, $\mu = 1$, $e = 0.45$, and $\delta = 0.1$ and keep control parameters fixed. To investigate the specific influence of the growth rate r on Q_{profit}, we vary r within a reasonable range while keeping all other parameters unchanged. The tested values of r are selected as 1.2, 1.4, 1.6, and 1.8, which cover the typical variation interval of this parameter in similar ecological-economic models. This parameter setting ensures that the simulation results can reflect the relationship between r and Q_{profit}.

As shown in Figure 9, varying r within a reasonable range (other parameters fixed) reveals two trends: First, profit (Q_{profit} increases gradually with r; second, optimal harvesting level (x_l^*) changes accordingly. These confirm a monotonic positive $r - Q_{profit}$ relationship and show that r adjusts optimal management (via x_l^*), indicating that boosting r raises returns but requires recalibrating x_l^* for sustainability. These results validate the analysis objective: Quantifying Q_{profit} and visualizing trends provides insights into how r shapes system economic performance and optimal management.

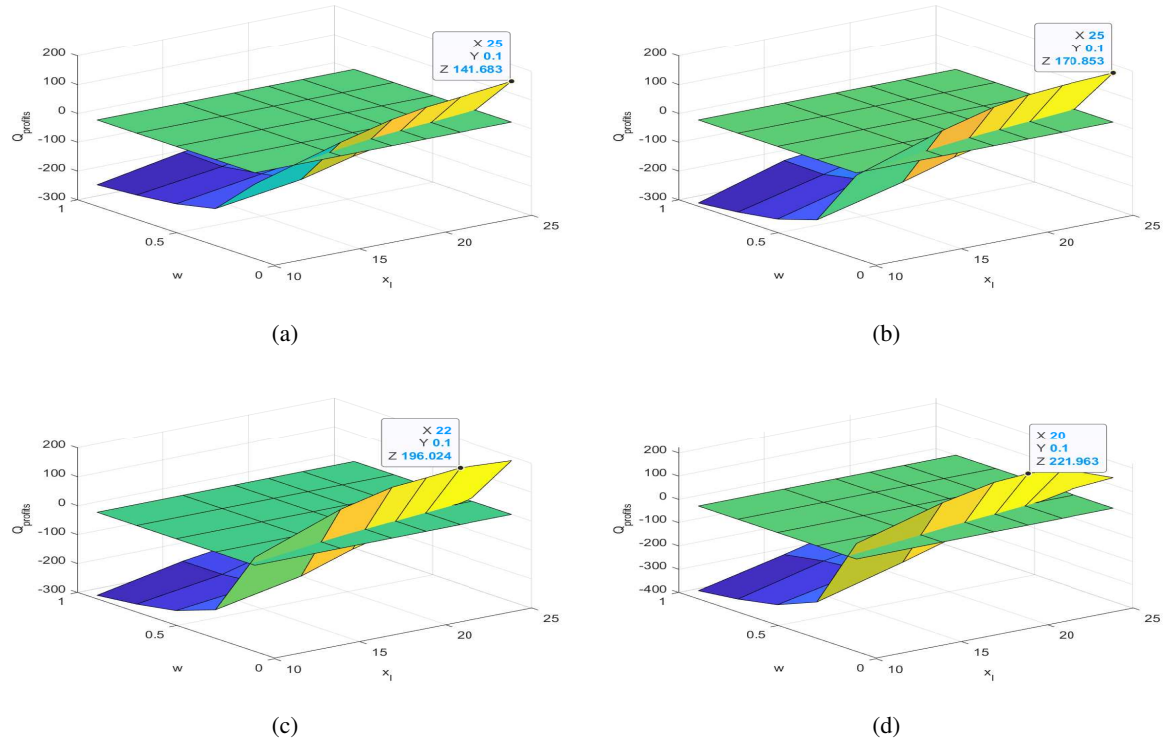

Figure 9. The change of profit Ψ_{Pro} with respect to r. (a) r=1.2, $\eta^* = 0.1$, $x_l^* = 25$, (b) r=1.4, $\eta^* = 0.1$, $x_l^* = 25$, (c) r=1.6, $\eta^* = 0.1$, $x_l^* = 22$, (d) r=1.8, $\eta^* = 0.1$, and $x_l^* = 20$.

4. Conclusions

Over-exploitation of natural resources can trigger a chain of risks in terms of ecology, economy, and public health. Therefore, sustainable resource management is imperative. To address this challenge, in this paper, we develop a state-dependent pulsed predator-prey model based on a weighted harvesting strategy, defining the intervention trigger as a linear combination of prey and predator densities ($h_l = \eta x + (1 - \eta)y$, $\eta \in [0, 1]$). This linear threshold design explicitly captures the inherent trophic interdependence between prey and predators, and it is particularly critical for predators vulnerable to the Allee effect-effectively overcoming the limitations of single-species thresholds that risk pushing such predators below their minimum viable population density and triggering irreversible extinction. Theoretical analysis reveals that the existence and stability of order-1 periodic solutions are critical indicators of a self-regulating, balanced ecosystem under rational harvesting control, while stable semi-trivial solutions (predator extinction) warn of ecological collapse driven by over-exploitation, especially for Allee-effect-prone predators. Furthermore, the constructed optimization framework has generated an economically optimal harvesting strategy that conforms to biological constraints, ensuring that the population remains above the minimum feasible reproduction threshold. Numerical simulations validate the theoretical conditions for order-1 periodic solutions and quantify the impact of the prey intrinsic growth rate r on management outcomes: Variations in r directly affect the maximum economic profit, the ecosystem-stabilizing optimal harvesting intensity, and the optimal weighting

coefficient η that balances species conservation (particularly for Allee-effect-vulnerable predators) and economic gains. Overall, this paper provides a theoretically grounded and practically operable framework for sustainable predator-prey ecosystem management, with the linear composite trigger offering a flexible tool for balancing trophic interactions, protecting Allee-effect-prone predators, and meeting human livelihood needs.

Author contributions

Jing Xu: Supervision, Writing–review and editing; Tao Zu: Software, Methodology and visualization. All authors have read and approved the final version of the manuscript for publication.

Use of Generative-AI tools declaration

The authors declare they have not used Artificial Intelligence (AI) tools in the creation of this paper.

Acknowledgements

This work was supported by the National Natural Science Foundation of China (No. 12401639, 62473134), the Nature Science Foundation of Hubei Province (No. 2024AFB170), Hubei Province University's outstanding young and middle-aged scientific and technological innovation team project (T2023020).

Conflict of interest

The authors declare no conflicts of interest in this paper.

References

1. B. Dennis, Allee effects: population growth, critical density, and the chance of extinction, *Nat. Resour. Model.*, **3** (1989), 481–538. https://doi.org/10.1111/j.1939-7445.1989.tb00119.x
2. F. Courchamp, L. Berec, J. Gascoigne, *Allee effects in ecology and conservation*, Oxford University Press, 2008. https://doi.org/10.1093/acprof:oso/9780198570301.001.0001
3. L. A. D. Rodrigues, D. C. Mistro, S. Petrovskii, Pattern formation, long-term transients, and the Turing-Hopf bifurcation in a space- and time-discrete predator-prey system, *Bull. Math. Biol.*, **73** (2011), 1812–1840. https://doi.org/10.1007/s11538-010-9593-5
4. W. C. Allee, O. Park, A. E. Emerson, T. Park, K. P. Schmidt, *Principles of animal ecology*, Philadelphia: Saunders, 1949. https://doi.org/10.5962/bhl.title.7325
5. P. Aguirre, E. González-Olivares, E. Sáez, Three limit cycles in a Leslie-Gower predator-prey model with additive Allee effect, *SIAM J. Appl. Math.*, **69** (2009), 1244–1262. https://doi.org/10.1137/070705210
6. U. Kumar, P. S. Mandal, Impact of additive Allee effect on the dynamics of an intraguild predation model with specialist predator, *Int. J. Bifur. Chaos*, **30** (2020), 2050239. https://doi.org/10.1142/S0218127420502399

7. S. Mandal, F. Al Basir, S. Ray, Additive Allee effect of top predator in a mathematical model of three species food chain, *Energy Ecol. Environ.*, **6** (2021), 451–461. https://doi.org/10.1007/s40974-020-00200-3
8. A. Arsie, C. Kottegoda, C. H. Shan, A predator-prey system with generalized Holling type IV functional response and Allee effects in prey, *J. Differ. Equations*, **309** (2022), 704–740. https://doi.org/10.1016/j.jde.2021.11.041
9. K. Mokni, M. Ch-Chaoui, Complex dynamics and bifurcation analysis for a Beverton-Holt population model with Allee effect, *Int. J. Biomath.*, **16** (2023), 2250127. https://doi.org/10.1142/S1793524522501273
10. X. Y. Xu, Y. Meng, Y. Y. Shao, Hopf bifurcation of a delayed predator-prey model with Allee effect and anti-predator behavior, *Int. J. Biomath.*, **16** (2023), 2250125. https://doi.org/10.1142/S179352452250125X
11. J. Zu, M. Mimura, The impact of Allee effect on a predator-prey system with Holling type II functional response, *Appl. Math. Comput.*, **217** (2010), 3542–3556. https://doi.org/10.1016/j.amc.2010.09.029
12. S. B. Hsu, T. W. Hwang, Y. Kuang, Global analysis of the Michaelis-Menten-type ratio-dependent predator-prey system, *J. Math. Biol.*, **42** (2001), 489–506. https://doi.org/10.1007/s002850100079
13. Y. Kuang, H. I. Freedman, Uniqueness of limit cycles in Gause-type models of predator-prey systems, *Math. Biosci.*, **88** (1988), 67–84. https://doi.org/10.1016/0025-5564(88)90049-1
14. A. D. Bazykin, *Nonlinear dynamics of interacting populations*, World Scientific, 1998. https://doi.org/10.1142/2284
15. D. Sen, A. Morozov, S. Ghorai, M. Banerjee, Bifurcation analysis of the predator-prey model with the Allee effect in the predator, *J. Math. Biol.*, **84** (2022), 7. https://doi.org/10.1007/s00285-021-01707-x
16. J. R. Beddington, R. M. May, The harvesting of interacting species in a natural ecosystem, *Sci. Am.*, **247** (1982), 62–69.
17. G. R. Dai, M. X. Tang, Coexistence region and global dynamics of a harvested predator-prey system, *SIAM J. Appl. Math.*, **58** (1998), 193–210. https://doi.org/10.1137/S0036139994275799
18. Y. F. Lv, R. Yuan, Y. Z. Pei, A prey-predator model with harvesting for fishery resource with reserve area, *Appl. Math. Model.*, **37** (2013), 3048–3062. https://doi.org/10.1016/j.apm.2012.07.030
19. M. Onana, B. Mewoli, J. J. Tewa, Hopf bifurcation analysis in a delayed Leslie-Gower predator-prey model incorporating additional food for predators, refuge and threshold harvesting of preys, *Nonlinear Dyn.*, **100** (2020), 3007–3028. https://doi.org/10.1007/s11071-020-05659-7
20. E. Liz, E. Sovranoa, Stability, bifurcations and hydra effects in a stage-structured population model with threshold harvesting, *Commun. Nonlinear Sci. Numer. Simul.*, **109** (2022), 106280. https://doi.org/10.1016/j.cnsns.2022.106280
21. H. J. Guo, L. S. Chen, The effects of impulsive harvest on a predator-prey system with distributed time delay, *Commun. Nonlinear Sci. Numer. Simul.*, **14** (2009), 2301–2309. https://doi.org/10.1016/j.cnsns.2008.05.010

22. L. F. Nie, Z. D. Teng, H. Lin, J. G. Peng, The dynamics of a Lotka-Volterra predator-prey model with state dependent impulsive harvest for predator, *Biosystems*, **98** (2009), 67–72. https://doi.org/10.1016/j.biosystems.2009.06.001

23. I. Noy-Meir, Stability of grazing systems: an application of predator-prey graphs, *J. Ecol.*, **63** (1975), 459–481. https://doi.org/10.2307/2258730

24. C. W. Clark, *Bioeconomic modelling and fisheries management*, New York: Wiley, 1985.

25. M. I. S. Costa, E. Kaszkurewicz, A. Bhaya, L. Hsu, Achieving global convergence to an equilibrium population in predator-prey systems by the use of a discontinuous harvesting policy, *Ecol. Model.*, **128** (2000), 89–99. https://doi.org/10.1016/S0304-3800(99)00220-3

26. Y. Tian, Y. Gao, K. B. Sun, Qualitative analysis of exponential power rate fishery model and complex dynamics guided by a discontinuous weighted fishing strategy, *Commun. Nonlinear Sci. Numer. Simul.*, **118** (2023), 107011. https://doi.org/10.1016/j.cnsns.2022.107011

27. Y. Tian, Y. Gao, K. B. Sun, Global dynamics analysis of instantaneous harvest fishery model guided by weighted escapement strategy, *Chaos Solitons Fract.*, **164** (2022), 112597. https://doi.org/10.1016/j.chaos.2022.112597

28. Y. Tian, Y. Gao, K. B. Sun, A fishery predator-prey model with anti-predator behavior and complex dynamics induced by weighted fishing strategies, *Math. Biosci. Eng.*, **20** (2023), 1558–1579. https://doi.org/10.3934/mbe.2023071

29. G. P. Pang, L. S. Chen, Periodic solution of the system with impulsive state feedback control, *Nonlinear Dyn.*, **78** (2014), 743–753. https://doi.org/10.1007/s11071-014-1473-3

30. J. Xu, Y. Tian, H. J. Guo, X. Y. Song, Dynamical analysis of a pest management Leslie-Gower model with ratio-dependent functional response, *Nonlinear Dyn.*, **93** (2018), 705–720. https://doi.org/10.1007/s11071-018-4219-9

31. J. Xu, M. Z. Huang, X. Y. Song, Dynamics of a guanaco-sheep competitive system with unilateral and bilateral control, *Nonlinear Dyn.*, **107** (2022), 3111–3126. https://doi.org/10.1007/s11071-021-07128-1

Appendix: Some definitions and lemmas

In this section, we introduce some definitions and lemmas about the geometric theory of the semi-continuous dynamical system.

Consider the semi-continuous dynamical system [29]

$$\left\{\begin{array}{l} \left.\begin{array}{l} \dfrac{\mathrm{d}x}{\mathrm{d}t} = P(x,y), \\ \dfrac{\mathrm{d}y}{\mathrm{d}t} = Q(x,y), \end{array}\right\} \quad if \;\; M(x,y) \neq 0, \\ \left.\begin{array}{l} \Delta x = E(x,y), \\ \Delta y = F(x,y), \end{array}\right\} \quad if \;\; M(x,y) = 0, \end{array}\right.$$

where $M(x,y)$ is called the impulsive set. Denote the impulsive map $\phi : (x,y) \to (x+\Delta x, y+\Delta y)$, i.e., $N(x,y) = \phi(M(x,y))$. Additionally, if $(x,y) \notin M(x,y)$, then the system develops under the regulation of $f(x,y) = (\frac{\mathrm{d}x}{\mathrm{d}t} = P(x,y), \frac{\mathrm{d}y}{\mathrm{d}t} = Q(x,y))$, which is similar to a continuous system.

Lemma A.1. *(Stability criterion [30]) The T_L period-1 solution $X(t) = (\xi(t), \eta(t))$ of the proposed model is orbitally asymptotically stable if the convergency ratio ρ_{γ_L} is less than one, where*

$$\rho_{\gamma_L} \triangleq \left| \frac{P^I_+[(1+\beta_y)\Phi_x - \beta_x\Phi_y] + Q^I_+[(1+\alpha_x)\Phi_y - \alpha_y\Phi_x]}{P^I\Phi_x + Q^I\Phi_y} \right| \exp\left(\int_{0^+}^{T} \left[\frac{\partial P}{\partial x} + \frac{\partial Q}{\partial y} \right]_{(\xi(t),\eta(t))} \right),$$

$P^I(Q^I)$ represents the value of $P(Q)$ at $L^-(\xi(T_L), \eta(T_L)) \in M_{imp}$, and $P^I_+(Q^I_+)$ represents the value of $P(Q)$ at $L(\xi(0^+), \eta(0^+)) \in N_{pha}$.

Next, the definition of the successor function is introduced.

Definition A.1. *(Successor function [30, 31]) Let M_{IMP} and N_{PHA} be two disjoint lines. Denote O' as the intersection point between N_{PHA} and x-axis (or y-axis if $N_{PHA} \cap$ x-axis=$\emptyset$). For a given $A_1 \in N_{PHA}$, the trajectory from A_1, passing through point A_2, intersects the impulsive set at the point A_3, then jumps to point $A_4 \in N_{PHA}$, and $A_4 = \phi(A3)$. Then, a type-I successor function f^I_{SOR} is defined by $f^I_{SOR} = d(A_4, O') - d(A_2, O')$, and a type-II function f^{II}_{SOR} is defined by $f^{II}_{SOR} = d(A_4, O') - d(A_1, O')$, as shown in Figure 10.*

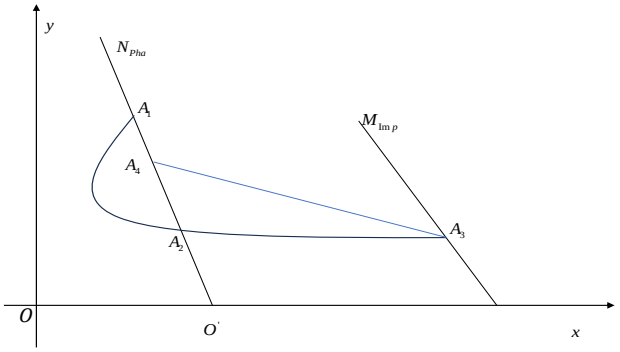

Figure 10. Schematic diagram of the successor function.